Int J Thermophys (2007) 28:1161–1180
DOI 10.1007/s10765-007-0221-z

Thermal Conductivity of Aqueous Sugar Solutions under High Pressure

M. Werner · A. Baars · F. Werner · C. Eder · A. Delgado

Received: 28 November 2006 / Accepted: 14 June 2007 / Published online: 21 August 2007
© Springer Science+Business Media, LLC 2007

Abstract Molecular energy transport in aqueous sucrose and glucose solutions of different mass fractions and temperatures is investigated up to 400 MPa, using the transient hot-wire method. The results reveal an increasing thermal conductivity with increasing pressure and decreasing mass fraction of sugar. No significant differences between sucrose and glucose solutions were observed. Different empirical and semi-empirical relations from the literature are discussed to describe and elucidate the behavior of the solutions with pressure. The pressure-induced change of the thermal conductivity of sugar solutions is mainly caused by an increase of the thermal conductivity and the decrease of molar volume of the water fraction. A simple pressure adapted mass fraction model permits an estimation of the thermal conductivity of the investigated solutions within an uncertainty of about 3%.

Keywords Aqueous · Density · Glucose · High pressure · Sucrose · Thermal conductivity · Transient hot-wire method

1 Introduction

High-pressure (HP) processing in the field of bio- and food technology is an innovative procedure that offers a variety of new possibilities. Treatments at pressures up to 1 GPa

M. Werner (✉) · C. Eder
Lehrstuhl für Fluidmechanik und Prozessautomation, Technische Universität München, Weihenstephaner Steig 23, Freising 85350, Germany
e-mail: mwerner@wzw.tum.de

A. Baars · A. Delgado
Lehrstuhl für Strömungsmechanik, Friedrich-Alexander-Universität Erlangen-Nürnberg, Erlangen 91058, Germany

F. Werner
Fachhochschule Weihenstephan, Freising 85350, Germany

enable the creation of new functional properties and structures of biomaterials through pressure-induced modifications of inter- and intramolecular interactions [1]. These changes can have an effect on macroscopic properties such as viscosity, and therefore on mass and energy transport during high-pressure treatment [2]. The state variable pressure permits new insights in the structural behavior of matter [3]. Furthermore, high-pressure processing of foods enables gentle preservation at moderate temperatures. In contrast to conventional thermal conservation processes at higher temperatures, essential food ingredients like vitamins and flavors can be almost completely maintained, while microorganisms and enzymes can be inactivated to an acceptable level [4, 5].

During pressurization, the pressure change propagates with the speed of sound, while in thermal processes, energy transport by diffusion and convection proves to be much slower. As biochemical reaction kinetics depend on pressure and temperature [6], high-pressure treatments should lead to a more homogeneous chemical and biochemical conversion and thus to homogeneous product quality.

However, investigations of Denys et al. [7], Pehl and Delgado [8, 9], and Pehl et al. [10] as well as Hartmann and Delgado [11], Delgado et al. [12], and Hartmann et al. [13] show that during the compression phase and holding time, inhomogeneous temperature fields occur in high-pressure chambers due to the spatial distribution of different media. Hence, diffusive and convective thermal transport processes among product, packaging, pressure transmitting fluid, and pressure vessel appear.

In order to understand and estimate thermo-fluid dynamics during high-pressure processes, a knowledge about thermophysical properties of the media involved as functions of temperature and pressure are indispensable. Other than the viscosity, density, and heat capacity, the thermal conductivity,

$$\lambda = -\dot{q}_i \frac{\partial T}{\partial x_i} \tag{1}$$

proves to be of high importance. Here, $\dot{q}_i$ represents the heat flux and $\partial T/\partial x_i$ the temperature gradient. Pressure-dependent thermal conductivity data for food and food ingredients are rare in the literature. Data for pure water have been provided by Bridgman [14], Lawson et al. [15], Kestin et al. [16], or IAPWS [17]. Food relevant aqueous salt solutions (NaCl and KCl) as well as several other salt solutions have been investigated by Nagasaka et al. [18], Abdulagatov and Magomedov [19, 20] as well as El'darov [21] over a large temperature range and at pressures up to 100 MPa. Denys and Hendrickx [22] report data for thermal conductivities of tomato paste and apple pulp up to 400 MPa.

Riedel [23] provided already thermal conductivity data for aqueous sucrose and glucose solutions at ambient pressure in the mass fraction range of dissolved sugar from $w = 0.1$ to 0.6 mass sugar/mass solution, and temperatures between 1.5 and 80°C, using the coaxial-cylinder method. The mentioned uncertainty of the measurements is about 1% and investigations show no significant differences between the data for sugar- and glucose solutions. Bubník et al. [24] suggested the correlation function,

$$\lambda = Aw + B \tag{2}$$

with

$$A = 5.466 \times 10^{-8}\ T^2 - 1.176 \times 10^{-5}\ T - 3.024 \times 10^{-3},$$

and

$$B = -7.847 \times 10^{-6}\ T^2 + 1.976 \times 10^{-3}\ T + 0.563$$

for the thermal conductivity calculation of these two sugar solutions that meet the experimental results of Riedel [23] within about ±1.2%.

In this contribution, the effect of pressure up to 400 MPa on the thermal conductivity of aqueous sucrose and glucose solutions is investigated experimentally for the first time. For this purpose, the transient hot-wire method is adapted to high-pressure application. To describe the dependences of pressure, temperature, and solute mass fraction, different empirical and semi-empirical relations are applied to the data. The interpretation of the results allows statements concerning the molecular behavior of sugar under pressure.

2 Materials and Methods

To date, different methods have been applied in the literature for experimental investigations of the thermal conductivity λ under pressure. For low viscosity liquids up to pressures of 1,200 MPa, Bridgman [14] and Lawson et al. [15] employed a steady-state coaxial-cylinder method. Denys and Hendrickx [22] used a modified transient hot-wire method for highly viscous foods (tomato paste, apple pulp) up to 400 MPa. While the first method involves a rather complex construction, the second one only enables the measurement of highly viscous media due to the thermal inertia of thermocouple probes. Furthermore, a calibration based on a water–agar-gel system is necessary for the latter device. In this work, the classic transient hot-wire method [25] is adapted for applications up to 400 MPa (see also Werner et al. [26]). A platinum wire of 25 μm diameter acts both as a fast heating source and a temperature sensor. This enables short measurement periods in order to reduce the influence of free convection. The thermal conductivity,

$$\lambda = \frac{\dot{q}}{4\pi} \left[\ln\left(t_2/t_1\right)/\left(T_2/T_1\right)\right] \tag{3}$$

is obtained by simplification of the Fourier differential equation [25]. The symbol t_i represents the time, T_i is the temperature, and $\dot{q}$ is the heat flow per unit wire length l_{Pt}. The heat flow,

$$\dot{q} = \frac{R_{\mathrm{Pt}}(T,\, p) I^2}{l_{\mathrm{Pt}}} \tag{4}$$

arises from the applied current I as well as from the temperature- and pressure-dependent wire resistance R_{Pt}. During measurements, a temperature increase,

$$\Delta T(t) = -\frac{\alpha_{\mathrm{Pt}}}{2\beta_{\mathrm{Pt}}} - T_{\mathrm{start}} - \sqrt{\frac{\Delta R_{\mathrm{Pt}}(t)}{R^0_{\mathrm{Pt}}(p)\cdot\beta_{\mathrm{Pt}}} + \left[\frac{\alpha_{\mathrm{Pt}}}{2\beta_{\mathrm{Pt}}} + T_{\mathrm{start}}\right]^2} \tag{5}$$

occurs in the wire. Here, α_{Pt} and β_{Pt} represent the temperature coefficients, $R^0_{\mathrm{Pt}}(p)$ is the pressure dependent reference resistance at $T = 0°\mathrm{C}$, T_{start} is the sample temperature just before measurement, and $\Delta R_{\mathrm{Pt}}(t)$ is the change in resistance of the platinum wire during the measurement.

Up to 400 MPa, investigations of Werner et al. [26] show that the influence of pressure on the electrical resistance of the hot-wire,

$$R_{\mathrm{Pt}}(T, p) = R^0_{\mathrm{Pt}}(p)(1 + \alpha_{\mathrm{Pt}}T + \beta_{\mathrm{Pt}}T^2) \tag{6}$$

can be considered by a pressure-dependent reference resistance R^0_{Pt} at 0°C.

2.1 Experimental Setup

The core of the experimental setup (Fig. 1) consists of a HP autoclave (a own custom-designed construction) with a maximum working pressure of 400 MPa, 28 mm inner diameter, 170 mm usable height, and 100 ml volume. A motor-driven piston pump (Sitec, Switzerland) generates the pressure, whereas the investigated fluid also acts as the pressure transmitting medium. Due to the small pump volume (4 ml), an additional valve between the pump and autoclave is necessary for reloads. The system pressure is measured by a pressure transducer (Brosa, Germany) with an uncertainty of ±1.75 MPa. A thermo-jacket, connected to a thermostat pump unit (Thermo Electron, Germany), encloses the autoclave and permits temperature settings between −20 and 70°C. The temperature in the vessel is detected by a digital thermometer (GMH3050, Greisinger GmbH, Germany) in combination with a Type T thermocouple (TC Mess- and Regeltechnik GmbH, Germany). The measurement uncertainty is ±0.13°C.

The electronics consists of an instrumental amplifier and a constant current source as well as a computer with a 16 bit data-acquisition-board (PCI-MIO-XE10, National Instruments). The analog outputs (−10 to 10 V) of the DAQ-board deliver the control-voltage for the current source and the reference voltage for the amplifier. The voltage drop across the hot-wire during measurement is compared with the reference value. The difference is amplified by a factor of 500 and converted digitally. The thermocouple, pressure transducer, and thermostat pump are linked to the computer. As measurement software, LabView (National Instruments) is used.

The hot-wire sensor (Fig. 1) is connected to a HP current feedthrough (Sitec) at the head seal package by a four-point connector. The upper end of the thin platinum wire (Ø 25 µm, length 100 mm) is soldered in a small brass bracket and the lower end in a small brass pin. To avoid a break of the wire due to deformation of the sensor at high-pressure conditions, the wire is fixed only at the upper end and stretched by

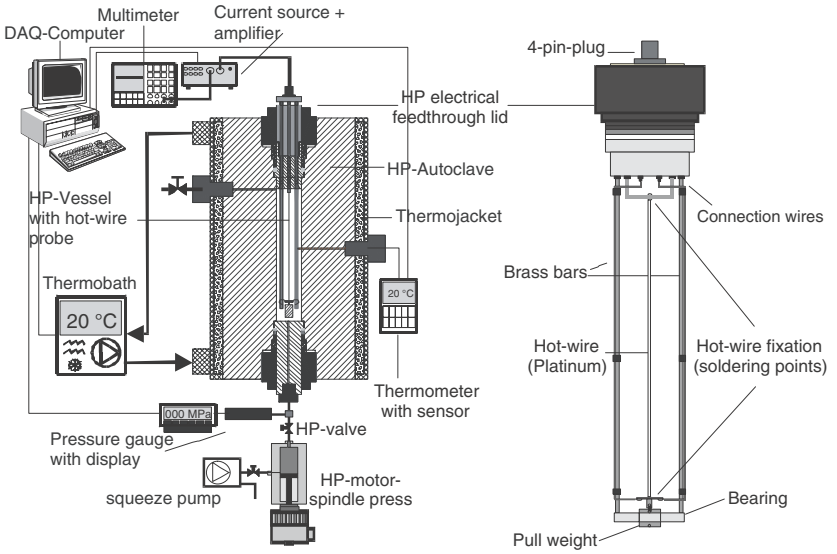

Fig. 1 Experimental setup and hot-wire probe

a weight. This is small to avoid a significant change in wire length. The influence of pressure on wire diameter and length are assumed to be small.

2.2 Experimental Procedure

After thermal equilibrium of the investigated fluid in the pressurized autoclave, the thermal conductivity measurement starts with a preset recording time t, current I, and reference voltage of the amplifier. Next, the DAQ system logs the voltage difference $\Delta U(t)$ at the platinum wire over the measurement period with a sample rate of 1 kHz and converts $\Delta U(t)$ to the electric resistance change of the wire,

$$\Delta R_{\mathrm{Pt}}(t) = \frac{\Delta U(t)}{I A}. \tag{7}$$

Here, A represents the amplification factor. In the next step, the temperature change $\Delta T(t)$ can be calculated by Eq. 5. Figure 2 depicts a characteristic run of temperature versus time (logarithmic plot). Section 1 of the curve represents the start-up phase including the preheating of the platinum wire. In Sect. 3, the temperature of the wire decreases due to the onset of free convection. For determination of the thermal conductivity by Eq. 3, the linear part of the curve (Sect. 2) is taken.

The standard uncertainty of the measurement system is about 4 $\mathrm{mW \cdot m^{-1} \cdot K^{-1}}$ and was derived on the basis of error propagation calculations, including all uncertainties of the involved system components.

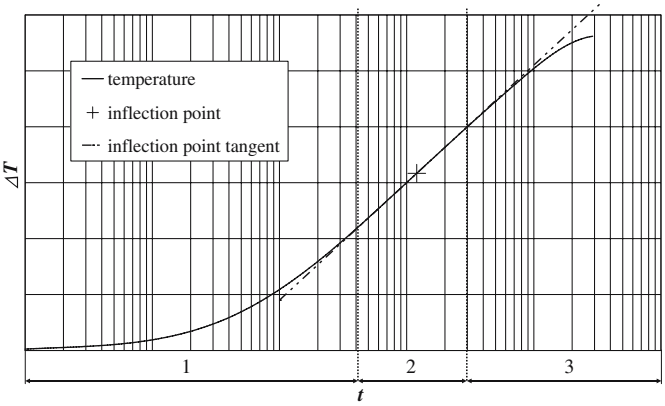

Fig. 2 Temperature-plot ΔT versus measurement time t

2.3 Sample Preparation

Aqueous sugar solutions of different mass fractions w (mass sugar/mass solution) are prepared using distilled water for analytical purposes (elec. conductivity $<0.05\,\mu S$, Normapur, VWR). The single fractions are weighed with a high precision laboratory balance (Sartorios, Germany, uncertainty: ± 0.003 g). Next, the mixtures are heated to 90°C and agitated with a magnetic stirrer to ensure complete dissolution of the sugar. After chilling the solutions were degassed by a water-jet vacuum pump. For preparation of glucose and sucrose solutions, we use pure, water free glucose and sucrose (biochemical grade, purity >99.5%, VWR). The uncertainty of the calculated mass fraction values w is lower than 0.5%.

3 Results

3.1 Validation

Figure 3 displays the data from this study and literature data for the thermal conductivity of water versus pressure up to 400 MPa. Despite the fact that polar liquids like water can lead to undefined uncertainties in thermal conductivity measurements with bare hot-wires and DC-heating currents [27], the averaged experimental results stay in good agreement with literature data. The standard deviation of the results amounts to a maximum value of about 7 $mW \cdot m^{-1} \cdot K^{-1}$. This scattering can be ascribed to the above named effect due to polarization of the liquid on the hot-wire surface what can result in a distortion of the measured voltage signal.

We assume that larger signal distortions have been reduced in these measurements according to large heating currents (large recorded voltage signals) and short measurement times what should limit the influence of this capacitance effect. The maximum deviation to measurements by Lawson et al. [15] and IAPWS [17] amounts to 2%.

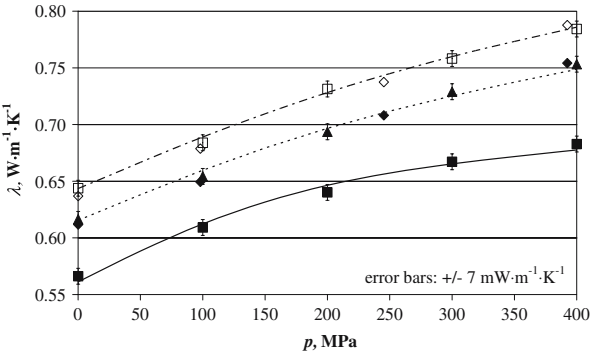

Fig. 3 Comparison among results from this study and data from the literature for $\lambda(p)$ of water at different temperatures and pressures: ■ 0.1°C/expt., ▲ 30°C/expt., □ 50°C/expt., ♦ 30°C/Lawson et al. [15], ◇ 50°C/Lawson et al. [15], — 0.1°C/IAPWS [17], ----- 30°C/IAPWS [17], - - - - - 50°C/IAPWS [17]

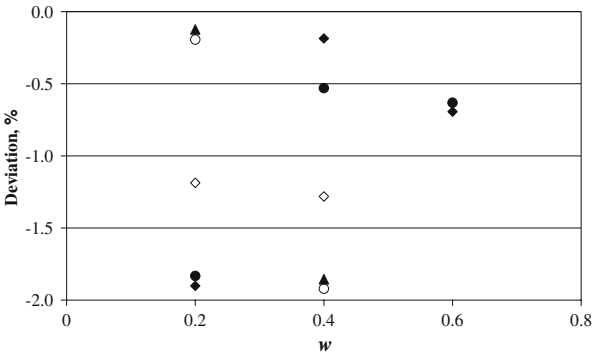

Fig. 4 Deviations between measured thermal conductivity λ of aqueous glucose (gluc) and sucrose (suc) solutions (different mass fractions w and temperatures) and literature data at ambient pressure: ♦ suc/20°C/Eq. 2, ● suc/20°C/Riedel [23], ○ gluc/20°C/Eq. 2, ▲ gluc/20°C/Riedel [23], ◇ gluc/40°C/Eq. 2

3.2 Thermal Conductivity of Aqueous Sugar Solutions

Figure 4 shows that the measured thermal conductivity of the sugar solutions at ambient pressure differs systematically up to −2% in relation to the data obtained by Riedel [23] and the correlation Eq. 2 from Bubník et al. [24]. Riedel [23] did not give any specifications about the purity of the used sugars. The deviations in this study may be attributed to charge separation and small impurities of the samples. The standard deviation of the results amounts to a maximum value of about 4 $\mathrm{mW \cdot m^{-1} \cdot K^{-1}}$ over the complete pressure range.

Figure 5 displays the relative thermal conductivity $\lambda_r(p) = \lambda(p)/\lambda(p_0)$ of aqueous glucose and sucrose solutions versus relative pressure $p_r = p/p_0$. The slopes of the isotherms decrease with pressure p and mass fraction w. In terms of relative values, the type of sugar show no significant effect on λ_r, while the absolute values of the thermal conductivity depend on w and T. From this finding, one could propose to describe the thermal conductivity by the product of two functions $\lambda = g(p)f(T)$. The absolute thermal conductivity does not indicate significant differences for the two types of sugar (sucrose, glucose).

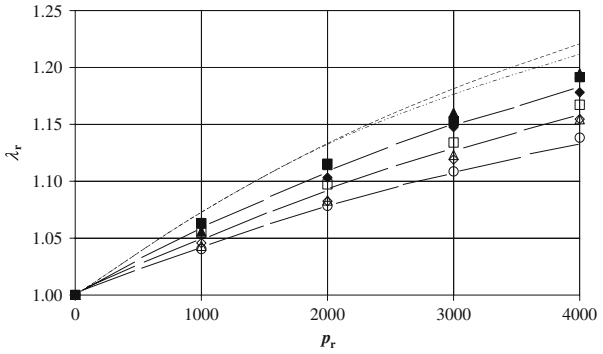

Fig. 5 Relative thermal conductivity λ_r of aqueous glucose (gluc) and sucrose (suc) solutions (different mass fractions w and temperatures) versus relative pressure p_r: ♦ suc/$w = 0.2/20°C$, ◇ suc/$w = 0.4/20°C$, ◯ suc/$w = 0.6/20°C$, ▲gluc/$w = 0.2/20°C$, ■ gluc/$w = 0.2/40°C$, △ gluc/$w = 0.4/20°C$, □ gluc/$w = 0.4/40°C$, —— water/20°C/[17], —··— water/40°C/[17]

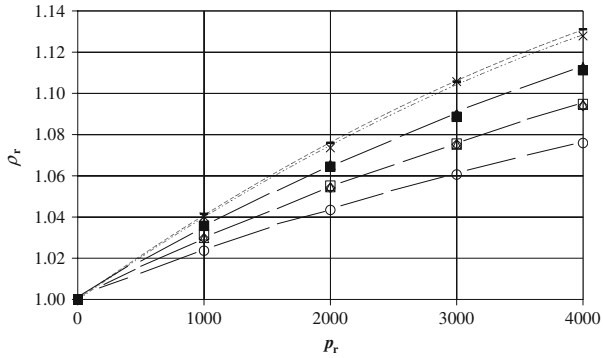

Fig. 6 Relative density ρ_r of aqueous glucose (gluc) and sucrose (suc) solutions (different mass fractions w and temperatures) versus relative pressure p_r: ♦ suc/$w = 0.2/20°C$, ◇ suc/$w = 0.4/20°C$, ◯ suc/$w = 0.6/20°C$, ▲ gluc/$w = 0.2/20°C$, ■ gluc/$w = 0.2/40°C$, △ gluc/$w = 0.4/20°C$, □ gluc/$w = 0.4/40°C$, —— water/20°C/[30], —··— water/40°C/[30]

A similar behavior with pressure can be observed for the relative density $\rho_r(p) = \rho(p)/\rho(p_0)$ of the investigated sugar solutions calculated by Eq. A1 in the Appendix. The slopes of the isotherms decrease also with pressure p and mass fraction w, but the increase is lower concerning the corresponding λ_r data. Furthermore, the temperature as well as the type of sugar has no significant effect on the relative quantity as Fig. 6 illustrates. The data indicate a reduced compressibility of the hydrated sugar molecules compared to water. The experimental results of λ_0 and $\lambda_r(p_r)$ as well as calculated data of ρ_0 and $\rho_r(p_r)$ are given in the Tables 1 and 2.

The two investigated types of sugar molecules differ in mass and size: the disaccharide sucrose has a mass and volume nearly twice as large as that for the monosaccharide glucose. For the case of equal mass fractions, the volume and mass of sugar in both solutions are almost the same, but they vary in number of dissolved molecules by a factor of approximately two. Hence, from the experimental results we can conclude

Table 1 Experimental data for thermal conductivity (λ_0, λ_r) and calculated densities (ρ_0, ρ_r; Eq. A1) for aqueous sucrose solutions at 20°C

	$w = 0.2$		$w = 0.4$		$w = 0.6$	
	$\lambda_0 = 0.524$ $(W \cdot m^{-1} \cdot K^{-1})$	$\rho_0 = 1081$ $(kg \cdot m^{-3})$	$\lambda_0 = 0.469$ $(W \cdot m^{-1} \cdot K^{-1})$	$\rho_0 = 1177$ $(kg \cdot m^{-3})$	$\lambda_0 = 0.402$ $(W \cdot m^{-1} \cdot K^{-1})$	$\rho_0 = 1287$ $(kg \cdot m^{-3})$
p_r	λ_r	ρ_r	λ_r	ρ_r	λ_r	ρ_r
1	1	1	1	1	1	1
1000	1.061	1.036	1.046	1.030	1.040	1.024
2000	1.103	1.065	1.082	1.054	1.078	1.043
3000	1.148	1.090	1.119	1.075	1.109	1.061
4000	1.178	1.112	1.155	1.094	1.138	1.076

that the compressibility and molecular energy transport of sucrose and glucose molecules do not differ significantly. From the similar behavior of density and thermal conductivity, one can conclude that a correlation between the transport quantity and the state variable exists. This will be discussed in the following section.

4 Discussion

For prediction of the thermal conductivity λ of pure liquids, mixtures, and aqueous solutions, a variety of empirical and semi-empirical equations exists in the literature. Table 3 shows an overview (Eqs. 8–18). The determination of the transport coefficient by molecular dynamic simulation, e.g. [28], is not considered here. In what follows, the temperature- and pressure-dependent data for the heat capacity and speed of sound for aqueous sucrose and glucose solutions and water are required. These are taken from Barbosa [29] and Wagner and Pruss [30], respectively. The density of water is obtained from [30] and the density of the sugar solutions is calculated by Eq. A1 in the Appendix. To the knowledge of the authors, only the expressions of Bridgman [14] and El'darov [21] (Eqs. 9 and 13, Table 3) have been applied to data for liquids under high pressure, in the latter case up to 50 MPa.

A first empirical expression for pure liquids has been given by Weber [31] in 1885. The quantity C in Eq. 8 in Table 3 denotes a constant, c_p is the specific heat capacity, ρ is the density, M is the molar mass, and δ represents a mean distance between the molecules. In 1923 Bridgman [14] published a relation (Eq. 9), which was derived from a simple physical picture, where the energy is transferred from molecule to molecule at the speed of sound u; R is the universal gas constant. The expression by Lawson et al. [15] (Eq. 10) is based on kinetic gas theory, which has been adopted to non-metal solids and liquids. Here, the energy is transferred by phonons at the speed of sound u. The mean free path l of the phonons is expressed by an empirical relation, containing the lattice constant a, the thermal expansion coefficient α, the Grüneisen constant γ_G and the absolute temperature T. Horrocks and McLaughlin [32] distinguish energy transfer due to vibration and Brownian motion of molecules. For each mechanism,

Table 2 Experimental data for thermal conductivity (λ_0, λ_r) and calculated densities (ρ_0, ρ_r; Eq. A1) for aqueous glucose solutions at 20 and 40°C

	$w = 0.2$, $T = 20$°C		$w = 0.4$, $T = 20$°C		$w = 0.2$, $T = 40$°C		$w = 0.4$, $T = 40$°C	
	$\lambda_0 = 0.534$ ($W \cdot m^{-1} \cdot K^{-1}$)	$\rho_0 = 1080$ ($kg \cdot m^{-3}$)	$\lambda_0 = 0.461$ ($W \cdot m^{-1} \cdot K^{-1}$)	$\rho_0 = 1173$ ($kg \cdot m^{-3}$)	$\lambda_0 = 0.555$ ($W \cdot m^{-1} \cdot K^{-1}$)	$\rho_0 = 1072$ ($kg \cdot m^{-3}$)	$\lambda_0 = 0.487$ ($W \cdot m^{-1} \cdot K^{-1}$)	$\rho_0 = 1164$ ($kg \cdot m^{-3}$)
p_r	λ_r	ρ_r	λ_r	ρ_r	λ_r	ρ_r	λ_r	ρ_r
1	1	1	1	1	1	1	1	1
1000	1.056	1.036	1.043	1.030	1.063	1.036	1.055	1.031
2000	1.114	1.065	1.083	1.055	1.115	1.064	1.090	1.055
3000	1.160	1.090	1.123	1.075	1.152	1.087	1.134	1.076
4000	1.194	1.113	1.155	1.095	1.191	1.111	1.161	1.095

Table 3 Relations for prediction of the thermal conductivity from literature

Ref.	Equation	Media	Eq. No.
Weber [31]	$\lambda = \mathrm{C}\frac{\rho c_\mathrm{p}}{\delta};\quad \delta = \left[\frac{M}{\rho}\right]^{1/3}$	Liquids	(8)
Bridgman [14]	$\lambda = 2\frac{\mathrm{R}u}{\delta^2};\quad \delta = \left[\frac{M}{\rho}\right]^{1/3}$	Liquids	(9)
Lawson et al. [15]	$\lambda = \frac{1}{3}\rho c_\mathrm{p} u l;\quad l = \frac{a}{\alpha\gamma T}$	Water	(10)
	$\lambda = \lambda_\mathrm{vib.} + \lambda_\mathrm{brown.}$		
Horrocks and McLaughlin [32]	$\lambda_\mathrm{vib.} = 2nP\nu l\mathrm{d}U/\mathrm{d}T$ $\lambda_\mathrm{brown.} = 2nkl\mathrm{d}U/\mathrm{d}T$	Liquids (argon, nitrogen, carbon monoxide, methane, benzene, carbon tetrachloride)	(11)
Vargaftik and Os'minin [34]	$\frac{\lambda}{\lambda_1} = \frac{c_\mathrm{p}}{c_{\mathrm{p},1}}\frac{\rho}{\rho_1}\left[\frac{M_1/\rho_1}{M/\rho}\right]^{1/3}$	Electrolyte solutions	(12)
El'darov [21]	$\frac{\lambda}{\lambda_1} = B\frac{\rho}{\rho_1}$	Aqueous KCl, NaCl, $CaCl_2$ sultions	(13)
Bäckström and Emblik [35], Comini et al. [36]	$\lambda(T) = (1-x_2)\lambda_1(T) + x_2\lambda_2(T)$	Aqueous food suspensions/solutions	(14)
Sutherland–Wassiljewa equation [38]	$\lambda = \frac{\lambda_1}{1+A_{12}(N_2/N_1)} + \frac{\lambda_2}{1+A_{21}(N_1/N_2)}$		(15)
Pandey and Mishra [37]	$A_{ij} = \frac{1}{4}\left[1+\left(\frac{\lambda_i}{\lambda_j}\right)^{1/2}\left(\frac{M_j}{M_i}\right)^{3/8}\right]^2$	Mixtures of organic liquids	(16)
Wilke [39]	$A_{ij} = \frac{1}{4}\left[1+\left(\frac{\lambda_i}{\lambda_j}\right)^{1/2}\left(\frac{M_j}{M_i}\right)^{1/4}\right]^2 \times\left[\frac{2M_j}{M_i+M_j}\right]^{1/2}$	Viscosity of gas mixtures	(17)
Rastorguev and Ganiev [40]	$V_1 > V_2$: $\lambda = \frac{\lambda_2 N_2}{N_2 + (2V_1/V_2 - 1)N_1} + \frac{\lambda_1 (2V_1/V_2 - 1)N_1}{N_2 + (2V_1/V_2 - 1)N_1}$ $V_2 > V_1$: $\lambda = \frac{\lambda_2 (2V_2/V_1 - 1)N_2}{N_1 + (2V_2/V_1 - 1)N_2} + \frac{\lambda_1 N_1}{N_1 + (2V_2/V_1 - 1)N_2}$ s	Aqueous solutions, solutions of organic liquids	(18)

they give an expression, where n represents the number of molecules per unit area in a liquid lattice, P is the probability of a collision of two vibrating molecules, ν is the frequency of vibration, k is the frequency of atom movement from one adjacent layer to the next, l is the distance between molecule planes, and $\mathrm{d}U/\mathrm{d}T$ is the heat capacity per molecule.

These first four expressions (only vibrational energy transport) predict an increase in thermal conductivity with increasing density, which corresponds to the findings in the last section. Equation 11 contains the density indirectly. This becomes apparent by extending the expression with length l and the mass of a single molecule. To apply these relations to solutions, the average molecular mass,

$$M = \left[\sum_{i=1}^{n} \frac{w_i}{M_i} \right]^{-1} \tag{19}$$

is calculated by considering the mass fraction w_i and the molecular mass M_i of the molecules involved. Bridgman's equation overestimates the thermal conductivity in relation to the measured data for sucrose solutions with increasing pressure and mass fraction. A maximum deviation of +48% is found at 400 MPa, 20°C, and $w = 0.6$. An improvement of the prediction can be obtained by introducing information to the relation in the form of referencing the thermal conductivity (a) to that of the solution at ambient pressure or (b) to the pressure-dependent thermal conductivity of the solvent. For (a), a maximum deviation of +27% and for (b) of −27% remain. By applying this technique to Eq. 8 of Weber [31] and Eq. 10 of Lawson et al. [15], the relations of Vargaftik and Os'minin [34] (Eq. 12) and El'darov [21] (Eq. 13) emerge. These will be discussed later. Gorbachev [33] proposed a further relation, which is also based on a model of oscillating molecules in a lattice. This contains the surface tension, which is unknown for sugar solutions in the investigated pressure range.

Apart from a more or less physical background, the expressions for thermal conductivity of mixtures differ in the type of parameters involved. Equations 12 and 13 include the thermal conductivities and other properties (density, heat capacity) of the solvent (index l) and the solution (no index). Here, the thermal conductivity of the mixture is obtained by scaling the thermal conductivity of the solvent with additional thermophysical values. The latter includes information about the solute fraction and intermolecular interactions.

The second group, Eqs. 14–18, contains the thermal conductivities (and densities—Eq. 18) of the pure components and considers the composition (mass or mole fractions). In general, solids have higher thermal conductivities in comparison to liquids due to the different intermolecular distances and conformations. Pure sugar exists only in a crystalline form. To apply the latter relations to sugar solutions, the thermal conductivity of sugar is obtained by regression to experimental data. Depending on the physical background of the expression, the received values reflect the intermolecular interactions between solvent and solute molecules as well as between solute molecules. For Eqs. 14–18, the thermal conductivities of sucrose and glucose are considered to be independent of pressure.

Vargaftik and Os'minin [34] gave a relation for aqueous electrolyte solutions which can be obtained by applying the expression of Weber [31] and referencing the thermal conductivity of the solution to the solvent. Hereby, one assumes the constant C to cancel out. For the investigated sugar solutions, a maximum deviation of 10% is found.

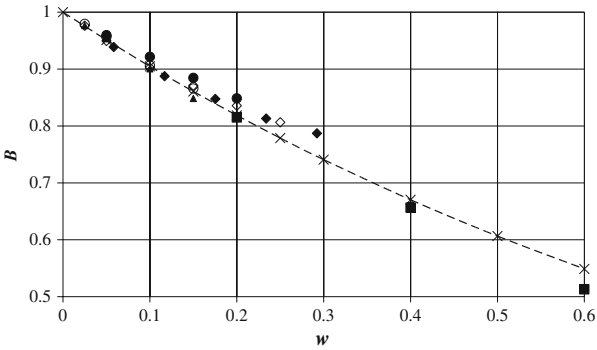

Fig. 7 Parameter B for different aqueous solutions versus mass fraction w: ♦ NaCl [18] ($T = 1$–$80°C$, $p_{max} = 40$ MPa), ◇ NaCl [19], ◯ $Sr(NO_2)_3$ [20], ▲ $SrCl_2$ [20], ($T = 20$–$100°C$, $p_{max} = 100$ MPa), • KCl–NaCl–$CaCl_2$ [21] ($T = 20$–$100°C$, $p_{max} = 50$ MPa), ■ sucrose expt. ($T = 20°C$, $p_{max} = 400$ MPa), △ glucose expt. ($T = 20°C$, $p_{max} = 400$ MPa), □ glucose expt. ($T = 40°C$, $p_{max} = 400$ MPa), —x— $\exp(-w)$

El'darov [21] proposed Eq. 13 to predict the thermal conductivity of aqueous salt solutions for pressures up to 50 MPa. This relation can be considered as an analog to that of Vargaftik and Os'minin [34] via Eqs. 8–10 (Weber, Bridgman and Lawson et al.). Except for density, all remaining properties are unified in the parameter B. El'darov does not give any relation for B, but he found this parameter to depend on the mass fraction of the dissolved substance.

Figure 7 depicts B versus the solute mass fraction for the investigated sugar solutions, as well as for salt solutions at various temperatures and pressures taken from the literature [18–21]. Parameter B is obtained from Eq. 13 by regression.

For the different kinds of solutes, different temperature and pressures, the data points of parameter B seem to follow a common trend. The progression characterizes a non-linear decrease with mass fraction. In a first approach, the function,

$$B = \exp(-w), \tag{20}$$

follows the trend of data. Equations 13 and 20 seem to provide a useful estimation of thermal conductivities for various aqueous solutions. Figure 8 depicts the deviations $[(\lambda_{model} - \lambda_{expt.})/\lambda_{expt.} \times 100\%]$ from experimental data as a function of mass fraction.

The maximum deviation for the NaCl-solution is 5.3%, and the maximum value for the investigated sugar solutions amounts to 9.5% at $w = 0.6$.

The simple empirical relation of Eq. 14 for aqueous food solutions/suspensions has been reported in [35, 36]. The experimental results of Riedel [23] and Eq. 2 from Bubník et al. [24] reflect also a linear relation between $\lambda_{solution}$ and w for glucose and sucrose solutions. The thermal conductivity λ_2 in Eq. 14 can be derived as λ_{sugar} from Eq. 2 for $w = 1$, assuming a linear relationship over the complete mass fraction range at constant temperature while λ_1 represents the thermal conductivity of water. The temperature-dependent thermal conductivity $\lambda_{sugar}(T)$ of dissolved sugar amounts to about $0.26\ W \cdot m^{-1} \cdot K^{-1}$ at atmospheric pressure and 0°C. Due to different molecu-

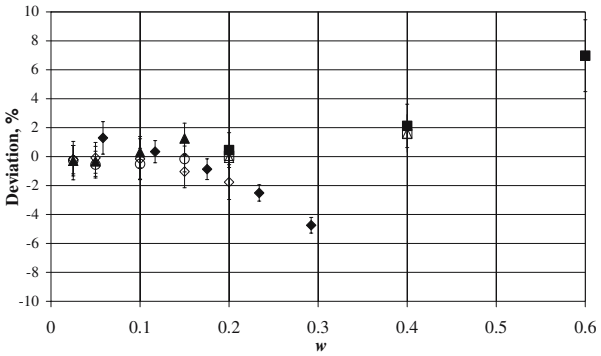

Fig. 8 Deviations between calculation by Eq. 13 and experiment for $B = \exp(-w)$ at high pressure: ♦ NaCl [18] (T = 1–80°C, p_{max} = 40 MPa), ◇ NaCl [19], ◯ $Sr(NO_2)_3$ [20], ▲ $SrCl_2$ [20], (T = 20–100°C, p_{max} = 100 MPa), ■ sucrose expt. (T = 20°C, p_{max} = 400 MPa), △ glucose expt. (T = 20°C, p_{max} = 400 MPa), □ glucose expt. (T = 40°C, p_{max} = 400 MPa)

lar interactions, a lower value could be expected with respect to crystallized matter ($\lambda_{sugar,\,crist} = 0.582\,W \cdot m^{-1} \cdot K^{-1}$ [24]). In this work, Eq. 14 is extended by the use of parameter pressure,

$$\lambda_{solution}(p, T, w) = (1 - w)\lambda_{H_2O}(p, T) + w\lambda_{sugar}(p_0, T) \tag{21}$$

where only the influence of pressure on the thermal conductivity of water is considered. The predicted values for aqueous sucrose and glucose solutions agree well (−0.5 to 3.6%) with the experimental results (Fig. 9).

Pandey and Mishra [37] apply the Sutherland–Wassiljewa equation (Eq. 15) [38] to predict the thermal conductivity and the diffusion coefficient of liquid mixtures. Wilke [39] uses the same relation to determine the viscosity of gas mixtures. This equation is based on the kinetic gas theory. Each author proposes an empiric relation for the Wassiljewa coefficient A_{ij}. Pandey and Mishra [37] used both empirical expressions (Eqs. 15 and 16) to calculate the thermal conductivities of binary organic liquid mixtures at ambient pressure. For the case of pressurized aqueous sugar solutions, a maximum deviation of about 5% (Eqs. 15 and 16, Fig. 10 and Eqs. 15 and 17, Fig. 11) is found.

Rastorguev and Ganiev [40] derived a relation for aqueous and organic solutions, based on the model by Horrocks and McLaughlin [32], Eq. 11. The former authors consider the probability of collisions of different types of molecules of molar volumes V_i of the pure substances and the corresponding mole fractions N_i. In this work, the molar volumes of sugar $V_{sugar} = M_{sugar}/\rho_{sugar}$ are estimated by the density of crystallized matter (data from [24]) without considering any pressure dependence. The comparison to measured data leads to a maximum deviation of 2.5% (Fig. 12).

The values calculated from Eqs. 14–18 for dissolved sugar are given in Table 4 and are much lower in comparison to those for the crystallized form ($\lambda_{sugar,crist.} = 0.582\,W \cdot m^{-1} \cdot K^{-1}$ at 0°C). They vary between 0.138 and 0.318 $W \cdot m^{-1} \cdot K^{-1}$. This appears reasonable due to the less rigid intermolecular interactions for liquids. The

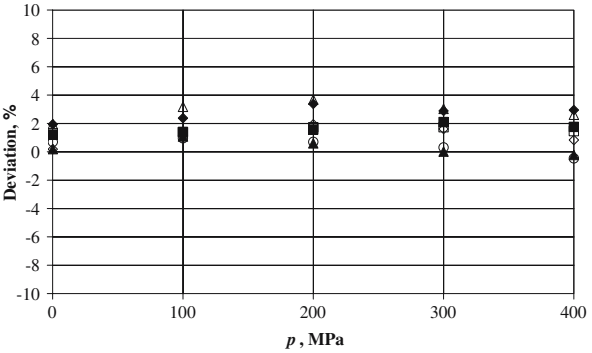

Fig. 9 Deviations between mass fraction model Eq. 14 and experimental thermal conductivity of sucrose and glucose solutions versus pressure p: ♦ suc/w = 0.2/20°C, ◇ suc/w = 0.4/20°C, ◯ suc/w = 0.6/20°C, ▲ gluc/w = 0.2/20°C, ■ gluc/w = 0.2/40°C, △ gluc/w = 0.4/20°C, □ gluc/w = 0.4/40°C (sucrose: $\lambda_{sugar} = 0.276\,W \cdot m^{-1} \cdot K^{-1}$, glucose 20°C: $\lambda_{sugar} = 0.276\,W \cdot m^{-1} \cdot K^{-1}$, glucose 40°C: $\lambda_{sugar} = 0.289\,W \cdot m^{-1} \cdot K^{-1}$)

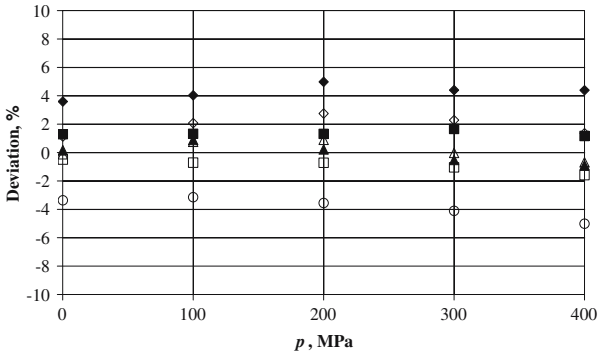

Fig. 10 Deviations between Sutherland–Pandey model Eqs. 15 and 16 and experimental thermal conductivity of sucrose and glucose solutions versus pressure p: ♦ suc/w = 0.2/20°C, ◇ suc/w = 0.4/20°C, ◯ suc/w = 0.6/20°C, ▲ gluc/w = 0.2/20°C, ■ gluc/w = 0.2/40°C, △ gluc/w = 0.4/20°C, □ gluc/w = 0.4/40°C (sucrose 20°C: $\lambda_{sugar} = 0.217\,W \cdot m^{-1} \cdot K^{-1}$, glucose 20°C: $\lambda_{sugar} = 0.222\,W \cdot m^{-1} \cdot K^{-1}$, glucose 40°C: $\lambda_{sugar} = 0.235\,W \cdot m^{-1} \cdot K^{-1}$)

assumed pressure independent thermal conductivities/molar volumes for dissolved sugar and the good agreement of Eq. 21 with experimental data confirm the behavior that dissolved sugar molecules undergo much smaller pressure-induced modifications with respect to water to affect the thermal energy transport. This is supported by the fact that water dissociates with increasing pressure [41], which leads to a denser packing (principle of LeChatellier), while sugar molecules remain intact. Furthermore, using density measurements of aqueous sucrose solutions, Eder and Delgado [42] found nearly constant partial molar volumes of sugar molecules up to pressures of 400 MPa and mass fractions of 0.65. Based on these findings, one can conclude that sugar molecules can be considered as rigid bodies in comparison to water. Hence, an increase in pressure in aqueous sugar solution leads to an increase in volume fraction of sugar

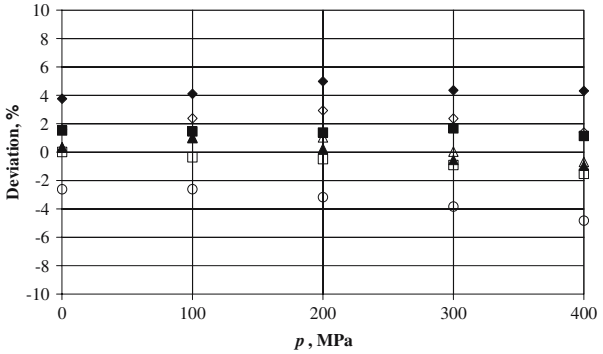

Fig. 11 Deviations between Sutherland–Wilke model Eqs. 15 and 17 and experimental thermal conductivity of sucrose and glucose solutions versus pressure p: ♦ suc/$w = 0.2/20°C$, ◇ suc/$w = 0.4/20°C$, ◯ suc/$w = 0.6/20°C$, ▲ gluc/$w = 0.2/20°C$, ■ gluc/$w = 0.2/40°C$, △ gluc/$w = 0.4/20°C$, □ gluc/$w = 0.4/40°C$ (sucrose 20°C: $\lambda_{sugar} = 0.138\,W \cdot m^{-1} \cdot K^{-1}$, glucose 20°C: $\lambda_{sugar} = 0.164\,W \cdot m^{-1} \cdot K^{-1}$, glucose 40°C: $\lambda_{sugar} = 0.174\,W \cdot m^{-1} \cdot K^{-1}$)

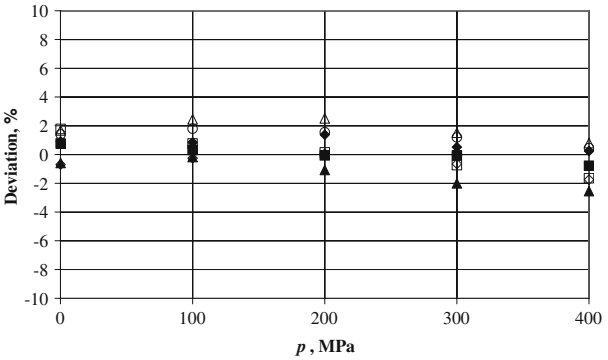

Fig. 12 Deviations between Rastorguev model Eq. 18 and experimental thermal conductivity of sucrose and glucose solutions versus pressure p: ♦ suc/$w = 0.2/20°C$, ◇ suc/$w = 0.4/20°C$, ◯ suc/$w = 0.6/20°C$, ▲ gluc/$w = 0.2/20°C$, ■ gluc/$w = 0.2/40°C$, △ gluc/$w = 0.4/20°C$, □ gluc/$w = 0.4/40°C$ (sucrose: $\lambda_{sugar} = 0.307\,W \cdot m^{-1} \cdot K^{-1}$, glucose 20°C: $\lambda_{sugar} = 0.318\,W \cdot m^{-1} \cdot K^{-1}$, glucose 40°C: $\lambda_{sugar} = 0.312\,W \cdot m^{-1} \cdot K^{-1}$)

molecules and therefore in V_{sugar}/V_{water}. From the relation of [40] follows, that with increasing pressure, the probability of collision between water molecules,

$$W_{water} = \frac{1}{1 + \left[2\frac{V_{sugar}}{V_{water}} - 1\right]\frac{N_{sugar}}{N_{water}}} \tag{22}$$

decreases, and that between sugar molecules $W_{sugar} = 1 - W_{water}$ increases. Since intermolecular energy transport and thermal conductivity are proportional to collision probability of molecules [32], sugar molecules influence more and more the energy transport in the solution. The thermal conductivity of dissolved sugar is lower than

Table 4 Comparison of calculated values for λ_{sugar} from Eqs. 14–18 for dissolved sugar

	λ_{sugar} ($W \cdot m^{-1} \cdot K^{-1}$)			
	Eq. 14	Eqs. 15 and 16	Eqs. 15 and 17	Eq. 18
Sucrose (20°C)	0.276	0.217	0.138	0.307
Glucose (20°C)	0.276	0.222	0.164	0.318
Glucose (40°C)	0.289	0.235	0.174	0.312

this of water and can be regarded as approximately independent on pressure. Hence, the absolute values of λ decrease with increasing N_{sugar}/N_{water}, V_{sugar}/V_{water}, and w.

5 Conclusion

The thermal conductivities of aqueous sucrose and glucose solutions have been investigated by a transient hot-wire method up to 400 MPa for different temperatures and solute mass fractions. The thermal conductivity of the investigated solutions increases with pressure while the slope of the isotherms decrease with increasing mass fraction of dissolved sugar and increasing pressure. The type of sugar (sucrose, glucose) shows no significant effect on λ. The density of the considered solutions shows a similar behavior as a function of the parameters investigated.

Different empirical and semi-empirical relations from literature have been applied to the data obtained at high pressure and discussed to

– describe λ as a function of pressure, temperature, and mass fraction,

– elucidate the correlation between density and thermal conductivity, and

– investigate the effect of pressure on the molecular transport of thermal energy.

Best agreement between experimental and calculated values was obtained using the simple empirical equation $\lambda_{solution}(p, T, w) = (1-w)\lambda_{H_2O}(p, T) + w\lambda_{sugar}(p_0, T)$.

Vargaftik and Os'minin [34] as well as El'darov [21] reported relations between density and thermal conductivity. In the latter case, the ratio of thermal conductivity solution/solvent is equal to a constant B times the density ratio of solution and solvent. To a first approximation, B is a function of mass fraction w, only, and proves to be independent of temperature, pressure, and the dissolved substance. By expressing B by $\exp(-w)$, a maximum deviation with experimental results of 9.5% is found.

The relation of Rastorguev and Ganiev [40] provides insight into the molecular behavior of a pressurized sugar solution. Here, a maximum deviation with experimental data of about 2.5% is found. The obtained results indicate that the pressure-induced changes in molecular energy transport in sugar solutions result from an increase of thermal conductivity and a decrease of molar volume of the water fraction with increasing pressure. The corresponding values of the dissolved sugar can be considered as con-

stant. Therefore, with increasing mass fraction, the thermal conductivity is governed more and more by the sugar fraction.

Appendix

Density data for aqueous sucrose and glucose solutions at ambient pressure for different mass fractions of sugar and temperatures are provided by Emmerich [43]. The density of sucrose solutions under high pressures up to 500 MPa is measured with high-pressure high accuracy densitometry (HP-HAD) introduced by Eder and Delgado [44]. We found an empirical formula, Eq. A1, which describes the density of the sugar solutions as a function of pressure, temperature, and mass fraction of dissolved sugar. Hereby, the polynomial equation given by Emmerich [43] for sucrose solutions at ambient pressure was extended by a pressure-dependent factor $k(p)$

$$\rho_{\text{solution}}(p, T, w) = \rho_{\text{H}_2\text{O}}(p_0, T)k(p) + \Delta\rho_{\text{sugar}}(p_0, T, w)k(p)^{-1} \tag{A1}$$

with $k(p) = \frac{\rho_{\text{H}_2\text{O}}{}^{(p)}}{\rho_{\text{H}_2\text{O}_{(0)}}}$.
The term $\Delta\rho_{\text{sugar}}$ for sucrose and glucose solutions is given by [43, 45]

$$\begin{aligned}\Delta\rho_{\text{sugar}}(p_0, T, w) = {} & b_{01}w + b_{02}w^2 + b_{03}w^3 + b_{04}w^4 + b_{05}w^5 + b_{06}w^6 \\ & + (b_{11}w^1 + b_{12}w^2 + b_{13}w^3 + b_{14}w^4 + b_{15}w^5)\tau \\ & + (b_{21}w + b_{22}w^2 + b_{23}w^3 + b_{24}w^4)\tau^2 \\ & + (b_{31}w + b_{32}w^2 + b_{33}w^3)\tau^3 \\ & + (b_{41}w + b_{42}w^2)\tau^4\end{aligned} \tag{A2}$$

with $\tau = (T - 20)/100$ and $b_{i,k}$

$b_{i,k}$ Sucrose						
i	$k = 1$	2	3	4	5	6
0	385.1761	135.3705	40.9299	−3.9643	13.4853	−17.2890
1	−46.2720	−7.1720	1.1597	5.1126	17.5254	
2	59.7712	7.2491	12.3630	−35.4791		
3	−47.2207	−21.6977	27.6301			
4	18.3184	12.3081				

$b_{i,k}$ Glucose						
i	$k = 1$	2	3	4	5	6
0	382.3089	122.8456	33.7382	−10.9724	15.7115	−17.0990
1	−55.131	−1.651	12.055	6.328	13.662	
2	75.748	−5.640	−2.244	−24.582		
3	−43.945	−16.701	−6.554			
4	0	0				

The density of water as a function of temperature and pressure can be obtained from Wagner and Pruss [30]. Thus, the densities of the sucrose solutions predicted by Eqs.

A1 and A2 are close to data of Eder and Delgado [42] measured with the HP-HAD method published at 20°C in [42] and the data presented by Barbosa [29]. In the first case the absolute deviations lie in a range of about +0.4 and −0.6% and in the second case between about +0.3 and −0.4% at pressures up to 600 MPa. Comparable results exist for the glucose solutions in relation to measured densities of Barbosa [29].

Equation A1 is also used for density predictions of the investigated aqueous salt solutions under high pressure, whereas $\Delta\rho_{\text{sugar}}$ is exchanged by $\Delta\rho_{\text{salt}}$. A comparison of the calculated results with density data of aqueous NaCl solutions up to 450 MPa in a temperature range from 5 to 60°C and mass fractions up to $w = 0.25$ (also measured by Eder and Delgado with HP-HAD published for 20°C in [42]) indicate an uncertainty of about ±1% related to the measured values.

Acknowledgments This work has been supported by the Deutsche Forschungsgemeinschaft (German Science Foundation) within the project DFG FOR 358/1-A3 and the Bundesministerium für Bildung und Forschung (Federal Ministry of Education and Research) within the project 0330098A.

References

1. C. Balny, P. Masson, K. Heremans, Biochim. Biophys. Acta **1595**, 3 (2002)
2. A. Baars, L. Kulisiewicz, R. Gebhardt, W. Doster, A. Delgado, *in Proceedings of the 4th International Symposium on the Food Rheology and Structure*, ETH Zurich (2006), pp. 283–287
3. K. Heremans, L. Smeller, Biochim. Biophys. Acta **1386**, 353 (1998)
4. M.G. Gaenzle, H.M. Ulmer, R.F. Vogel, J. Food Sci. **66**, 1174 (2001)
5. I. Indrawati, L.R. Ludikhuyze, A.M. van Loey, M.E. Hendrickx, J. Agric. Food Chem. **48**, 1850 (2000)
6. B.A. Bauer, D. Knorr, J. Food Eng. **68**, 329 (2005)
7. S. Denys, A.M. van Loey, M.E. Hendrickx, Innov. Food Sci. Emerg. Technol. **1**, 5 (2000)
8. M. Pehl, A. Delgado, *Advances in High-pressure Bioscience and Biotechnology* (Springer, Heidelberg, 1999), pp. 519–522
9. M. Pehl, A. Delgado, *Trends in High Pressure Bioscience and Biotechnology* (Elsevier, Amsterdam, 2002), pp. 429–435
10. M. Pehl, F. Werner, A. Delgado, Exp. Fluids **29**, 302 (2000)
11. Chr. Hartmann, A. Delgado, Biotechnol. Bioeng. **79**, 94 (2002)
12. A. Delgado, Chr. Hartmann, R. Winter, *Advances in High Pressure Bioscience and Biotechnology II* (Springer, Berlin, Heidelberg, New York, 2003), pp. 459–464
13. Chr. Hartmann, J.P. Schuhholz, P. Kitsubun, N. Chapleau, A. Le Bail, A. Delgado, Innov. Food Sci. Emerg. Technol. **5**, 399 (2004)
14. P.W. Bridgman, *The Physics of High Pressure*, 2nd edn. (G. Bell & Sons, London, 1949), pp. 307–329
15. A.W. Lawson, R. Lowell, A.L. Jain, J. Chem. Phys. **30**, 643 (1959)
16. J. Kestin, J.V. Sengers, B. Kamgar-Parsi, J.M.H. Levelt Sengers, J. Phys. Chem. Ref. Data **13**, 175 (1984)
17. IAPWS, Revised Release on the IAPS Formulation 1985 for the Thermal Conductivity of Ordinary Water Substance, vol. 23 (International Association for the Properties of Water and Steam, London, 1998)
18. Y. Nagasaka, H. Okada, J. Suzuki, A. Nagashima, Ber. Bunsen-Ges. Phys. Chem. **87**, 859 (1983)
19. I.M. Abdulagatov, U.B. Magomedov, Int. J. Thermophys. **15**, 401 (1994)
20. I.M. Abdulagatov, U.B. Magomedov, Int. J. Thermophys. **20**, 187 (1999)
21. V.S. El'darov, High Temp. **41**, 327 (2003)
22. S. Denys, M.E. Hendrickx, J. Food Sci. **64**, 709 (1999)
23. L. Riedel, Chem. Eng. Technol. **21**, 340 (1949)
24. Z. Bubník, P. Kadlec, D. Urban, M. Bruhns, *Sugar Technologists Manual* (Bartens, Berlin, 1995), p. 155
25. R. Greger, A. Delgado, H.J. Rath, in *Proceedings of the IUTAM Symposium Microgravity Fluid Mechanics* (Springer, Berlin, Heidelberg, 1992), pp. 511–515

26. M. Werner, A. Baars, A. Delgado, *6. Dresdner Sensor-Symposium – Sensoren für zukünftige Hochtechnologien und Neuentwicklungen für die Verfahrenstechnik*, vol. 20 (W.E.B. Universitätsverlag, Dresden, 2003), p. 37
27. M.L.V. Ramires, J.M.N.A. Fareleira, C.A. Nieto de Castro, M. Dix, W.A. Wakeham, Int. J. Thermophys. **14**, 1119 (1993)
28. H. Sigurgeirsson, D.M. Heyes, Mol. Phys. **101**, 469 (2003)
29. R.D. Barbosa, Ph.D. thesis, University of Florida, Gainesville (2003), p. 203
30. W. Wagner, A. Pruss, J. Phys. Chem. Ref. Data **31**, 387 (2002)
31. H.F. Weber, Berlin. Ber. **2**, 809 (1885)
32. I.K. Horrocks, E. McLaughlin, Trans. Faraday Soc. **56**, 206 (1960)
33. M.Y. Gorbachev, Phys. Chem. Liq. **40**, 395 (2002)
34. N.B. Vargaftik, Y.P. Os'minin, Teploenergetika **3** (1956)
35. E.H.M. Bäckström, E. Emblik, *Kältetechnik*, vol. 3 (Verlag G. Braun, Karlsruhe, 1965), p. 498
36. G. Comini, C. Bonacina, S. Barina, Bull IIR **3**, 163 (1974)
37. J.D. Pandey, R.K. Mishra, Phys. Chem. Liq. **43**, 49 (2005)
38. C.C. Li, AiChE J. **22**, 927 (1976)
39. C.R. Wilke, J. Chem. Phys. **18**, 577 (1950)
40. Y.L. Rastorguev, Yu.A. Ganiev, Inz.-Fiz. Zh. **14**, 689 (1968)
41. V.M. Stippl, A. Delgado, T.M. Becker, Innov. Food Sci. Emerg. Technol. **5**, 285 (2004)
42. C. Eder, A. Delgado, in *Proceedings of the 7th International Conference on Optical Technol., Optical Sensors & Measuring Techniques* (AMA Service GmbH, Wunstorf, 2006), pp. 3.1–3.6
43. A. Emmerich, Zuckerindustrie **119**, 20 (1994)
44. C. Eder, A. Delgado, in *Lasermethoden in der Strömungsmesstechnik, 12 Fachtagung*, ed. by B. Ruck, A. Leder, D. Dopheide (GALA e.V., Karlsruhe, 2004), pp. 44.1–44.7.
45. H. Bettin, A. Emmerich, F. Spieweck, H. Toth, Zuckerindustrie **123**, 341 (1998)